JAEA-Technology
2016-040
DOI:10.11484/jaea-technology-2016-040

Neutronic Characteristic of HTTR Fuel Compact with Various Packing Models of Coated Fuel Particle

Hai Quan HO, Yuki HONDA, Minoru GOTO and Shoji TAKADA

Department of HTTR
Oarai Research and Development Center
Sector of Nuclear Science Research

March 2017

Japan Atomic Energy Agency

日本原子力研究開発機構

JAEA-Technology

本レポートは国立研究開発法人日本原子力研究開発機構が不定期に発行する成果報告書です。
本レポートの入手並びに著作権利用に関するお問い合わせは、下記あてにお問い合わせ下さい。
なお、本レポートの全文は日本原子力研究開発機構ホームページ（http://www.jaea.go.jp）
より発信されています。

国立研究開発法人日本原子力研究開発機構 研究連携成果展開部 研究成果管理課
〒319-1195 茨城県那珂郡東海村大字白方 2 番地4
電話 029-282-6387, Fax 029-282-5920, E-mail:ird-support@jaea.go.jp

This report is issued irregularly by Japan Atomic Energy Agency.
Inquiries about availability and/or copyright of this report should be addressed to
Institutional Repository Section,
Intellectual Resources Management and R&D Collaboration Department,
Japan Atomic Energy Agency.
2-4 Shirakata, Tokai-mura, Naka-gun, Ibaraki-ken 319-1195 Japan
Tel +81-29-282-6387, Fax +81-29-282-5920, E-mail:ird-support@jaea.go.jp

JAEA-Technology 2016-040

Neutronic Characteristic of HTTR Fuel Compact with Various Packing Models of Coated Fuel Particle

Hai Quan HO※, Yuki HONDA, Minoru GOTO＋and Shoji TAKADA

Department of HTTR,
Oarai Research and Development Center,
Sector of Nuclear Science Research,
Japan Atomic Energy Agency
Oarai-machi, Higashiibaraki-gun, Ibaraki-ken

(Received December 21, 2016)

To study the packing effects of the truncated coated fuel particle (CFP) on the criticality for the High Temperature engineering Test Reactor (HTTR), four alternative models including the truncated uniform model, the non-truncated uniform model, the truncated random model and the non-truncated random model for the arrangement of CFP in fuel compact were used, and the neutronic and criticality calculation were performed by using Monte Carlo MCNP6 code with ENDF/B-VII.1 cross section library. The results showed that the infinite multiplication factors (k_{inf}) in the truncated models were lower than those of the non-truncated models regardless of the uniform or random arrangement, and the four factors in the four-factor-formula showed that the difference of k_{inf} was mainly attributed to the resonance escape probability. The difference in resonance escape probability is caused by the increase of capture reactions in the resonance region as the influence of spatial-self-shielding-effect. It is because the equivalent kernel diameter of the CFP for the truncated model is smaller than that of the non-truncated model.

Keywords; HTTR, Coated Fuel Particle (CFP), Truncated CFP, Spatial Self-shielding Effect, MCNP6

＋ Small-sized HTGR Research and Development Division, HTGR Hydrogen and Heat Application Research Center
※ Post-Doctoral Fellow

様々な被覆粒子燃料充填モデルにおける HTTR 炉心の核特性評価

日本原子力研究開発機構　原子力科学研究部門
大洗研究開発センター　高温工学試験研究炉部

Hai Quan HO※, 本多 友貴, 後藤 実+, 高田 昌二

（2016 年 12 月 21 日　受理）

高温工学試験研究炉（HTTR）の臨界特性に対する被覆粒子燃料（CFP）のトランケーション（切欠き）の影響を調べるため、燃料コンパクト中の CFP の配列に関する 4 つの異なるモデル、すなわち、規則配列でトランケーションの有無のモデル、不規則配列でトランケーションの有無のモデルを作り、モンテカルロコード MCNP6、ENDF/B-VII.1 ライブラリを使って臨界計算を実施した。この結果、トランケーションありのモデルの無限実効増倍率 k_{inf} は、トランケーション無しの場合と比較して小さくなり、規則・不規則配列に関係しないことを明らかにした。さらに、4 因子公式の 4 因子の比較により、k_{inf} の違いが主に共鳴を逃れる確率によるものであることを明らかにした。また、共鳴を逃れる確率の違いは CFP のトランケーションモデルの等価直径が小さくなり、自己遮蔽効果の影響により共鳴領域で捕獲反応が増加するために生じることを明かにした。

大洗研究開発センター：〒311-1393　茨城県東茨城郡大洗町成田町 4002
＋　高温ガス炉水素・熱利用研究センター　小型高温ガス炉研究開発ディビジョン
※　博士研究員

Contents

目　次

List of tables

List of figures

1. Introduction

High-Temperature engineering Test Reactor (HTTR)[1] is the first Japanese High-Temperature Gas-cooled Reactor (HTGR) established in the Oarai Research and Development Center of Japan Atomic Energy Agency (JAEA). HTTR is a 30-MW_{th} prismatic type reactor, helium gas cooled and graphite moderated with the outlet temperature up to 950^{o}C. Coated Fuel Particles (CFPs) play an important role in the inherent safety feature of the HTTR design. However, the random distribution of the CFPs in the fuel compact makes the simulation of the HTTR become more complicated.

Nowadays, even though the supercomputers are powerful to enable the Monte-Carlo simulation of complex nuclear systems, there is a difficulty to simulate exactly the stochastic arrangement of CFPs in the HTGR in general as well as the HTTR in particular. In order to deal with the stochastic media, the Statistical Geometry model (STG) was developed and embedded into MVP code[2] by JAEA. The STG model had been validated with a good agreement between the calculation results by MVP code and the experiment results from the first criticality of the HTTR[3].

Currently, the numerical code MCNP^{TM} with the latest MCNP6 version[4] is one of the most well-known and popular Monte-Carlo codes for validation of nuclear systems. However, there is a remarkable challenge for evaluating the HTTR by using MCNP code due to the fact that it does not provide an appropriate function for modeling stochastic media of the fuel compact. For simplification, the uniform placement of the CFPs in lattice geometry was often used. For example, the CFPs are located in the infinite or finite cubical lattice[5]. The difference between the infinite and finite lattices is that in the case of the infinite model the CFPs can be truncated at the surface of the fuel, whereas in the case of the finite model there are no truncated CFPs at the surface of the fuel. Due to the simplification, the uniform model was widely applied in the calculations for the HTTR, such as benchmark evaluation of HTTR[6] using MCNP code.

The previous approaches for packing CFPs in the HTGR can be divided into two categories; one has truncated CFPs and the other has no truncated CFPs. The critical results showed that the truncation models make the multiplication factor differ significantly in comparison with the non-truncation models. For example, the previous study[7] showed the numerical results of MCNP5 calculation for the NGNP prismatic core design[8], in which the truncation model gave lower k_{eff} of about 260 pcm than the non-truncation model. The evaluation by MCNPX for GT-MHR[9] also showed about 550 pcm different in the k_{eff}, with the truncation model giving the lower value than that of non-truncation model. Another study[10] performed the burnup calculation for HTR prismatic fuel block using MCB5 code[11]; at the beginning-of-cycle (BOC) the truncation model presented lower k_{eff} value than that of non-truncation model, about 200 pcm for low packing fraction and 500 pcm for

high packing fraction. Unfortunately, the explanation for the difference between the truncation and non-truncation models was often omitted in the previous studies. Therefore the physical effect of the truncated CFPs to the criticality of the systems could not be understood clearly.

It should be mentioned that the previous benchmarks for the whole core of HTTR overestimated the k_{eff} by about 1.0 %Δk/k corresponding up to approximately 10 cm difference of the control rod position (ΔCR) between the calculation and measurement. It means that the change of only 0.1 %Δk/k (or 100 pcm) in k_{eff} makes the control rod position need to be changed by about 1 cm. The standard deviations of 0.1 %Δk/k (or 100 pcm) and ΔCR of 1 cm for the k_{eff} and the control rod position, respectively, are also required for the benchmark of HTTR not only in the calculation but also in the experiment. On the other hand, it is necessary to keep the control rod of metallic component in a high position of reactor core during operation. The highly accurate prediction technology of control rod position has been pursued. This technology is expected useful to reduce the design margin for core design to improve the economy of commercial HTGR. Therefore, even if the uncertainty caused by the effect of truncated CFP is small, it is necessary to be estimated for the actual evaluation of the HTTR.

The purpose of this study is to show the effect of truncated CFPs to the criticality of the specified HTTR fuel not only in the uniform arrangement but also in the random arrangement of CFP. Hence, 4 different models were used including the truncated uniform arrangement, the non-truncated uniform arrangement, the truncated random arrangement and the non-truncated random arrangement. The impact of the truncated CFP on the criticality of the systems was investigated in detail to understand the physical phenomenon obviously. The criticality and neutronic calculations were carried out by using the latest version MCNP6 and the ENDF/B-VII.1 cross-section library.

2. Design of HTTR

A schematic view of the HTTR is shown in Fig. 2.1. The 2.3-m-diameter, 2.9-m-high prismatic core consists of 30 fuel columns with 5 stacking fuel blocks per each column. The fuel block is a graphite hexagonal block, with 36 cm in width across flat and 58 cm in height as presented in Fig. 2.2. There are 31 or 33 fuel rods in each fuel block. Each fuel rod consists of 14 fuel compacts, in which about 13000 CFPs are stochastically embedded in an annular graphite matrix. The uranium enrichments in the HTTR core vary from 3 to 10 wt%, in which the fuel blocks containing high enrichment are located at the top and outer region of the

core to reduce the maximum power density during high-power operation. Detail specifications of the HTTR fuel design are shown in Table 2.1.

3. Models of HTTR fuel compact

To investigate the effect of the truncation of CFPs on the criticality of HTTR reactor, four models of CFPs arrangement are shown in this section as shown in Fig. 3.1. In the first two models (a) and (b), the effect of truncated CFPs is investigated in the cases of uniform arrangement. After that, the last two models (c) and (d) are used to show the truncation effect for the random arrangement.

3.1 Uniform with truncation

First, a CFP was placed in the center of a cubical cell. The length of the cubic was calculated to keep the volume packing fraction of 30%. Next, the cubical cell including the CFP in the center was expanded with repeated geometry feature. After that, the infinite universe containing single cubical lattice was filled in the annular fuel compact. This is the simplest method to model the distribution of the CFPs; however, the CFPs are truncated at the inner and outer surface of the fuel compact as can be observed from Fig. 3.1(a).

3.2 Uniform with non-truncation

This method is the same as the method mentioned above except the truncated CFPs at the boundary of fuel compact were visually eliminated. Then, the number of CFPs in each fuel compact was adjusted so as to remain the volume packing fraction of 30%. The simulated fuel compact of this model is shown in Fig. 3.1(b).

3.3 Random with truncation

In order to model the random arrangement of the CFPs, a computer program has been developed to generate a number of random points in a box[12]. Each random point was used as the center of a corresponding CFP. The fuel compact was then filled by the box lattice containing a number of random CFPs inside. The

cross-section of this model is shown in the Fig. 3.1(c). It can be seen that the random distribution of CFPs was presented explicitly; however, the CFPs were still truncated at the inner and outer surface of fuel compact.

3.4 Random with non-truncation

The simulation result of this model is shown in Fig. 3.1(d). In this model, a computer program was also developed to generate a number of random points, however, in an annular geometry. The inner and outer diameters of the annular geometry were the same as those of the fuel compact. Therefore, when the annular lattice was filled in the fuel compact, there were no truncated CFPs at the surface of the fuel. As a result, this model could not only model exactly the random arrangement of the CFPs but also remain their spherical geometry.

4. Calculation model and conditions

The single fuel block model using in this study is shown in Fig. 4.1. The block geometry was surrounded by a reflective boundary condition. The enrichment of uranium was about 6 wt%, which is the average uranium enrichment in the HTTR. The neutronic and criticality calculations were performed by the MCNP6 code and the ENDF/B-VII.1 library. The uniform temperature of 293.6K for neutron cross-section was used. In the calculation, the number of neutrons per cycle and the number of active cycles were 50,000 and 1000 (excluding 50 skip cycles), respectively, to achieve a standard deviation of about 0.0001 (10 pcm). The k_{inf} was evaluated for the four CFP packing models as shown in Fig. 3.1.

5. Result and discussion

In the first step, the criticality calculations were performed for the fuel block using the uniform with/without truncation models as shown in Fig. 3.1(a) and 3.1(b). As shown in Fig. 3.1(a), the number of truncated CFPs could be visually counted, taking possession of approximately 10 percent of the total CFPs in

the fuel compact. Therefore, it is expected that significant amount of the truncated CFPs can affect the criticality of the system. Table 5.1 shows the difference of k_{inf} between the truncated and non-truncated models for the uniform arrangement. The result showed that the difference of k_{inf} between the truncated model and non-truncated model was about 550 pcm.

In the cases of random arrangement as presented in Fig. 3.1(c) and 3.1(d), the number of truncated CFPs could be changed because of the arbitrary intersection between the CFPs and compact boundary. Therefore, 10 independent input files (corresponding to 10 differently random arrangements of CFPs) were prepared, 5 inputs for the truncated model and 5 inputs for the non-truncated model. The comparison of k_{inf} between the truncated and non-truncated models in the cases of random arrangement is shown in Table 5.2. The truncation models gave lower k_{inf} than that of the non-truncation model, from about 50 pcm to 200 pcm (120 pcm on average). It should be mentioned that the difference was at least 5 times larger than the standard deviation of the k_{inf} (σ = 10 pcm). Therefore, it is acceptable to discuss the difference between the two random models physically.

It can be seen that the k_{inf} of truncated models decreased not only in the cases of uniform arrangement but also in the cases of random arrangement. In order to explain the difference in k_{inf} between truncated and non-truncated models, four factors in the four-factor-formula were calculated. They were reproduction factor (η_T), thermal utilization factor (f), resonance escape probability factor (p) and fast fission factor (ε). Tables 5.3 and 5.4 showed the comparison of the four factors in the cases of uniform and random arrangement, respectively. It can be seen that the higher k_{inf} in the non-truncation models was mainly attributed to the resonance escape probability (p factor), with the non-truncation models giving a higher value of about 0.1% and 0.3% for random and uniform arrangements, respectively. It means that more neutrons were succeeded in slowing down to the thermal energies region resulted in larger k_{inf} in the cases of non-truncation models.

The change of resonance escape probability p can be explained from Fig. 5.1 which illustrated the equivalent kernel diameter of a truncated CFP in the uniform model. It can be seen that the equivalent kernel diameter of a truncated CFP is smaller than that of a normal CFP. And because of up to 10% CFPs is truncated in the surface of the fuel, it makes the average kernel diameter in the cases of truncation model significantly smaller than that of non-truncation model. The decrease of equivalent kernel diameter increased the capture of the fuel in the resonance region as the influence of spatial-self-shielding-effect[13]. The spatial-self-shielding-effect is independent of the random effect, where the criticality is decreased by random arrangement of CFPs. In case of the spatial-self-shielding-effect it makes the k_{inf} decrease with the decrease of equivalent CFPs diameter.

Figs. 5.2 and 5.3 present the comparison of the capture reaction rate between truncated and non-truncated

model in the cases of uniform and random arrangement, respectively. It can be seen that due to the spatial-self-shielding-effect the cases of truncation models (smaller equivalent kernel diameter) gave slightly higher capture reaction rate in comparison with non-truncation models with a larger equivalent kernel diameter. The increase of neutron capture decreased the thermal neutron flux, leading to lessen the k_{inf} in the case of truncation model. The results can also be clearly understood from the comparison of the neutron flux in resonance region between truncated and non-truncated models as illustrated in Figs. 5.4 and 5.5. The non-truncation models gave higher neutron flux at resonance region due to smaller capture reaction rate in this region.

6. Conclusion

The numerical investigation was carried out for various arrangements of CFP in fuel compact of the HTTR, including the uniform arrangement with/without truncated CFP and the random arrangement with/without truncated CFP. The criticality and neutronic calculations were performed for the HTTR prismatic block model by using the MCNP6 code and the ENDF/B-VII.1 cross-section library.

The impact of truncated CFPs on neutronic characteristic was investigated for both the uniform and random arrangements. The results showed that the truncated models gave lower k_{inf} than those of non-truncated models, regardless of the uniform or random arrangement of the CFPs. In the case of uniform arrangement, about 10% of CFPs were truncated at the surface of the fuel compact, resulting in k_{inf} reduction of about 550 pcm. The decrease of k_{inf} became smaller in the case of random arrangement due to the fact that less amount of CFP was truncated in this case.

The investigation of four factors in the four-factor-formula showed that the change k_{inf} was dominantly attributed to the resonance escape probability (p). The difference in resonance escape probability is because the equivalent kernel diameter of the CFP in the truncated model is smaller than that in the non-truncated model, leading to increase the capture reactions in the resonance region as the influence of spatial-self-shielding-effect. It makes the k_{inf} decrease for the truncated CFP model in comparison with non-truncated CFP model.

It was found that the truncation of CFP affected the neutronic characteristic and thereby leads to change the multiplication factor of the HTTR fuel block model. Physically, the difference in k_{inf} between the truncated and non-truncated CFP models can be smaller in the whole core calculations due to the fact that other core

regions, such as a side reflector, have lower spatial importance. However, as mentioned before, the control rod position sensitively depends on the k_{eff} of the HTTR, namely 0.1 %Δk/k (100 pcm) change in the k_{eff} causes 1 cm change in the control rod position. Therefore, further analysis for the whole core is necessary to investigate the physical effect of the truncated CFPs on the criticality of the HTTR more clearly.

References

1. Saito S., et al., Design of high temperature engineering test reactor (HTTR). JAERI 1332, 1994, 247p.
2. Mori, T., Nakagawa, M., MVP/GMVP: General Purpose Monte Carlo Codes for Neutron and Photon Transport Calculations Based on Continuous Energy and Multigroup Methods. JAERI-Data/Code 94-007, 1994, 388p.
3. Naoki, N., et al., Characteristic test of initial HTTR core. Nuclear Engineering and Design, 233, 2004, pp.283-290.
4. Goorley T., et al., Initial MCNP6 Release Overview. Nuclear Technology, 180, 2012, pp.298-315.
5. Brown, F.B., Martin, W.R., Stochastic geometry capability in MCNP5 for the analysis of particle fuel. Ann. Nucl. Energy, 31, 2004, pp.2039-2047.
6. John D. Bess and Nozomu F., Benchmark Evaluation of Start-Up and Zero-Power Measurements at the High-Temperature Engineering Test Reactor. Nuclear Science and Engineering, 178, 2014, pp.414-427.
7. Brown, F.B., et al., Stochastic geometry and HTGR modeling with MCNP5. Monte Carlo 2005 Topical Meeting – The Monte Carlo Method: Versatility Unbounded in a Dynamic Computing World, Chattanooga, Tennessee, April 17–21, 2005.
8. MacDonald P.E., et al., NGNP Preliminary Point Design – Results of the Initial neutronics and Thermal-Hydraulic Assessment During FY-03. INEEL/EXT-03-00870. Idaho National Engineering and Environmental Laboratory, 2003.
9. Jakova J., Talamo A., Criticality assessment for prismatic high temperature reactors by fuel stochastic Monte Carlo modeling. Ann. Nucl. Energy, 35, 2008, pp.856-860.
10. Kepisty, G., Monte Carlo burnup in HTR system with various TRISO packing. Ann Nucl. Energy, 92, 2016, pp.419-430.
11. Cetnar, J., et al., MCB: a continuous energy Monte Carlo Burnup simulation code. "Actinide and Fission Product Partitioning and Transmutation", EUR 18898 EN, OECD/NEA, 1999, pp.523-527.

12. Torabi Ardakani A., et al., Comparative modeling of stochastic versus regular arrangement of TRISO particles in HTTR. Progress in Nuclear Energy, 78, 2015, pp.291-296.

13. Dan Gabriel Cacuci., et al., Handbook of Nuclear Engineering, Vol II, 2010, pp.972-973.

14. Fujimoto, N., et al., Annular core experiments in HTTR`s start-up core physics tests. Nucl. Sci. Eng., 150, 2005, pp.310-321.

15. Minoru G., et al., Long-term high-temperature operation of the HTTR. Nuclear Engineering and Design, 251, 2012, pp.181-190.

Table 2.1 Fuel design of HTTR

Item	Value
Graphite block	
Material	IG-110
Density (g/cm^3)	1.75
Impurity (ppm)	<1 (Boron equivalent)
Fuel rod	
Outer diameter (cm)	3.4
Length (cm)	54.6
Number of fuel compact	14
Fuel compact	
Outer diameter (cm)	2.6
Inner diameter (cm)	1.0
Length (cm)	3.9
Volume packing fraction of CFP	0.3
Coated fuel particle	
Kernel diameter (μm)	600
Fuel kernel material	UO_2
Enriched uranium (wt%)	3.0-10.0
Kernel density (g/cm^3)	10.61
Coating material	PyC/PyC/SiC/PyC
Layer thickness (μm)	60/30/25/45

Table 5.1 Comparison of k_{inf} between truncation and non-truncation models in case of uniform arrangement ($1\sigma = 0.0001$ or 10pcm)

Truncation	Non-truncation	Δk (pcm)
1.49236	1.49784	548±14

Table 5.2 Comparison of k_{inf} between truncation and non-truncation models in case of random arrangement ($1\sigma = 0.0001$ or 10pcm)

Case	Truncation	Non-truncation	Δk (pcm)
#1	1.49052	1.49149	
#2	1.49034	1.49177	
#3	1.49041	1.49230	(50 ~ 200)±14
#4	1.49059	1.49143	
#5	1.49010	1.49113	

Table 5.3 Difference of the four factors between truncation and non-truncation models in case of uniform arrangement

Factor	Truncation	Non-truncation	Difference (%)
η_T	1.90311	1.90308	0.00
f	0.98998	0.99009	0.01
p	0.73028	0.73234	0.28
ε	1.10913	1.10989	0.07

Table 5.4 Difference of the four factors between truncation and non-truncation models in case of random arrangement arrangements (#1)

Factor	Truncation	Non-truncation	Difference (%)
η_T	1.90308	1.90307	0.00
f	0.99001	0.99001	0.00
p	0.72869	0.72945	0.10
ε	1.10993	1.11014	0.02

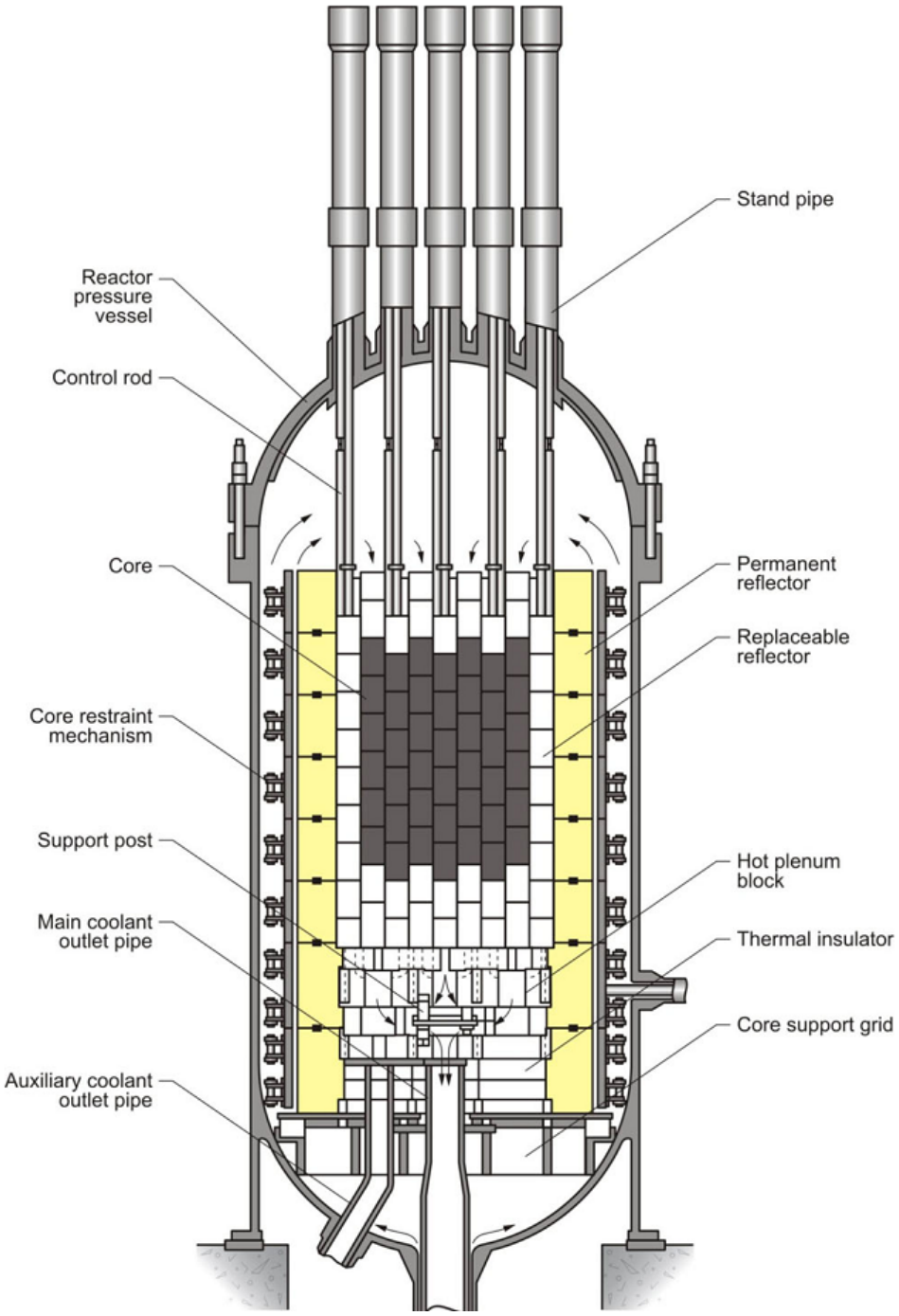

Fig. 2.1 Schematic view of HTTR[14)]

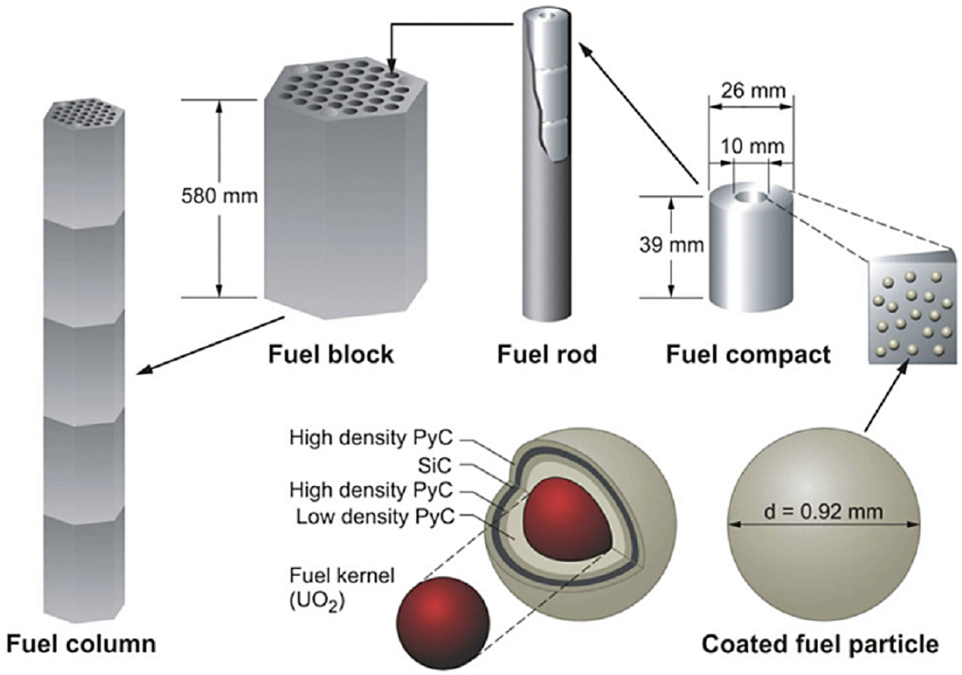

Fig. 2.2 HTTR fuel design[15)]

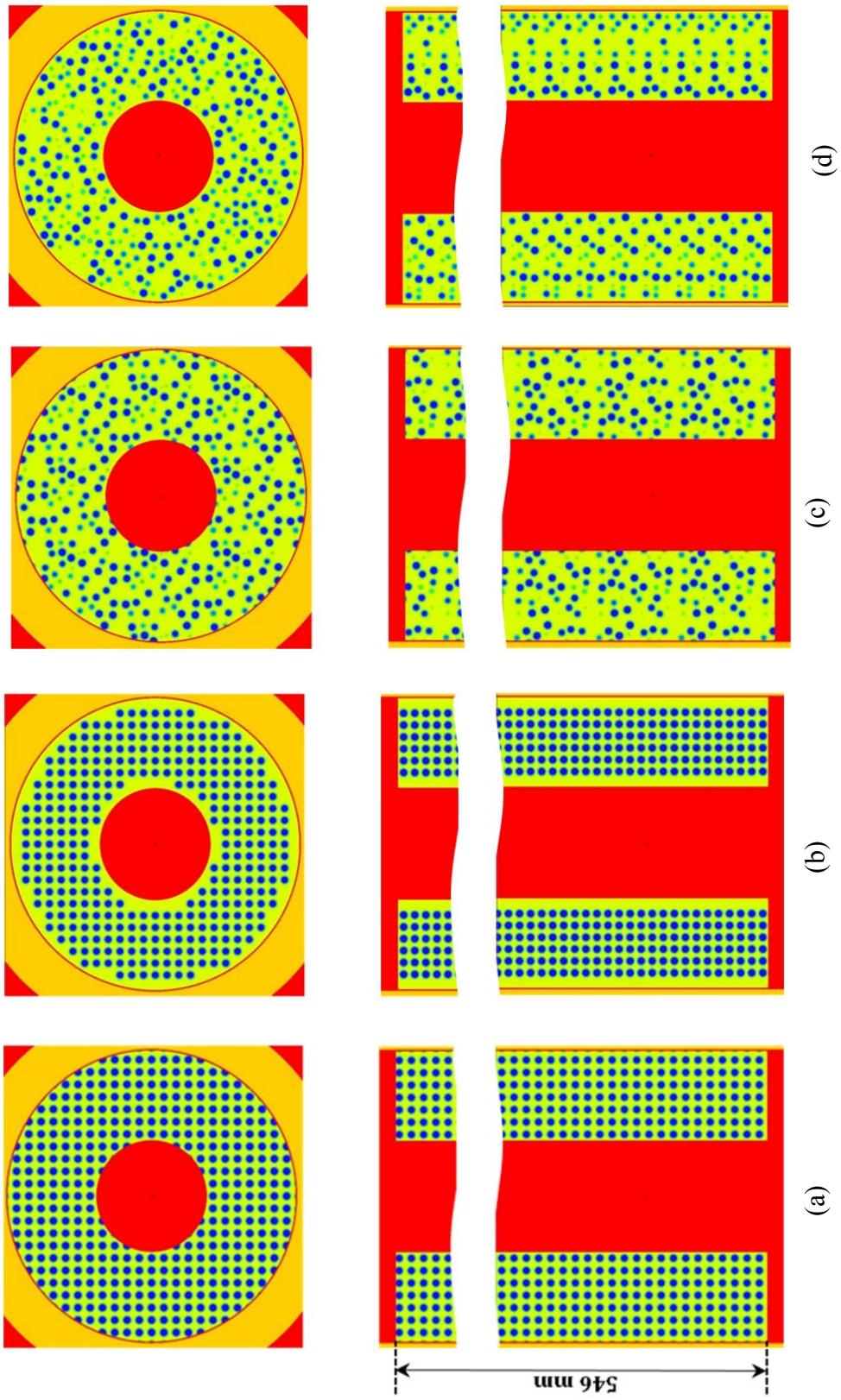

Fig. 3.1 Various arrangements of CFPs in the fuel compact plotted by MCNP6; (a) truncated uniform, (b) non-truncated uniform, (c) truncated random, (d) non-truncated random

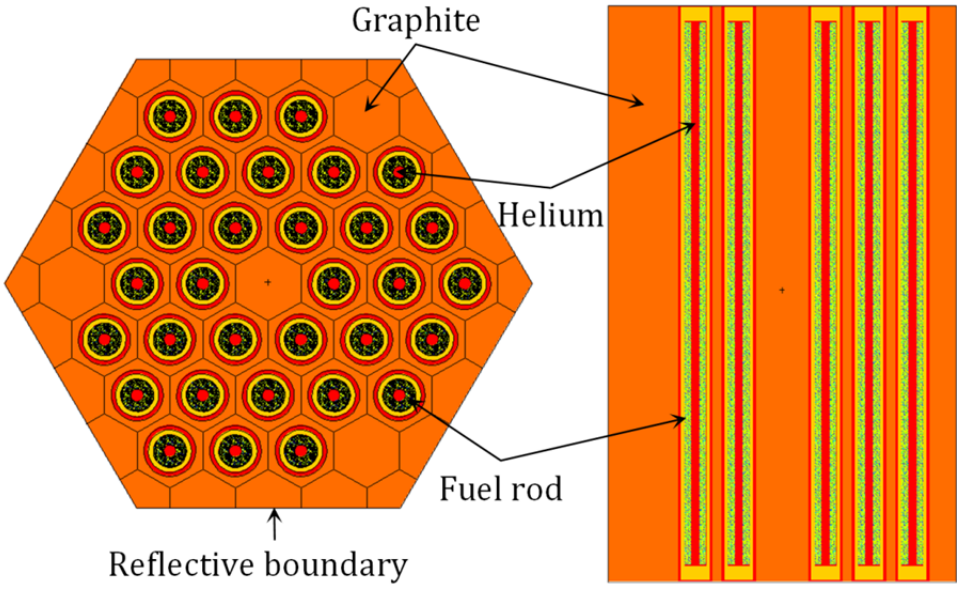

Fig. 4.1 HTTR block model plotted by MCNP6

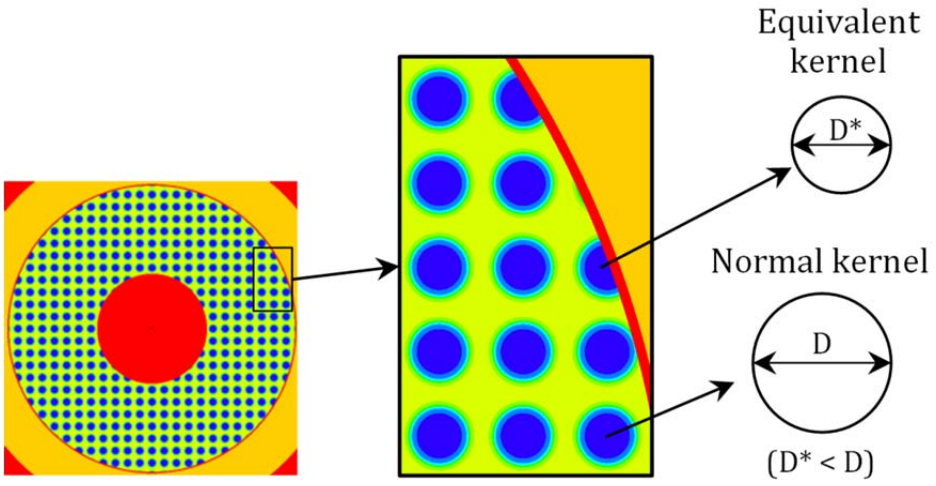

Fig. 5.1 Equivalent fuel kernel of truncated CFP compared to normal CFP

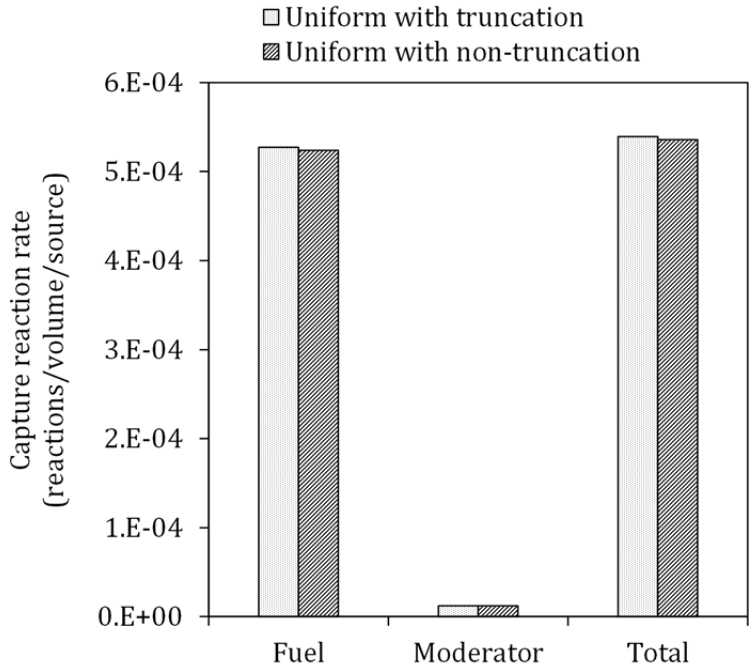

Fig. 5.2 Comparison of capture reaction rate between truncation and non-truncation models in the cases of uniform arrangement

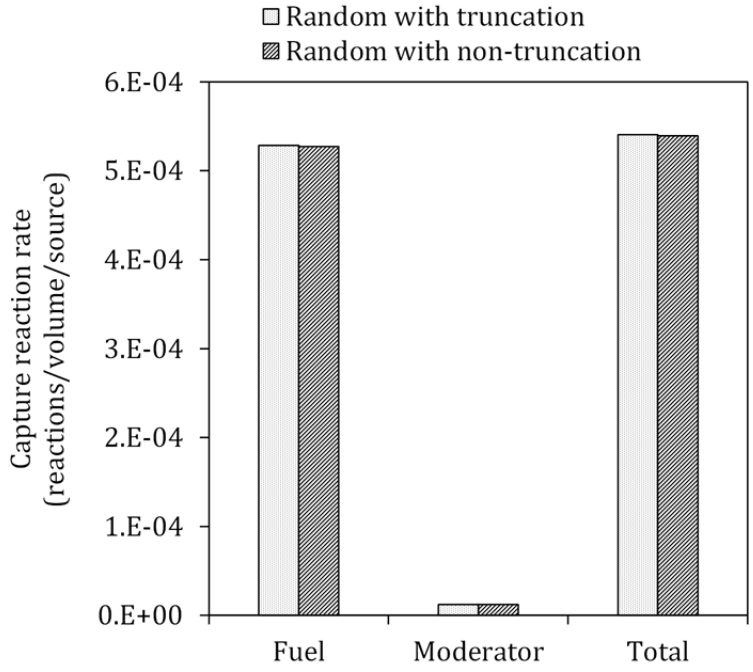

Fig. 5.3 Comparison of capture reaction rate between truncation and non-truncation models in the cases of random arrangement (#1)

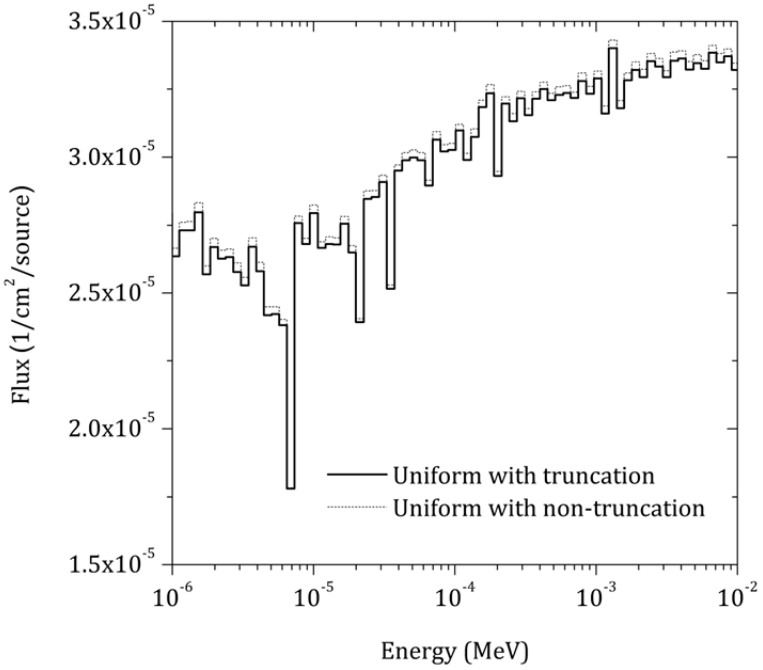

Fig. 5.4 Comparison of neutron flux in the resonance region between truncation and non-truncation models in the cases of uniform arrangement

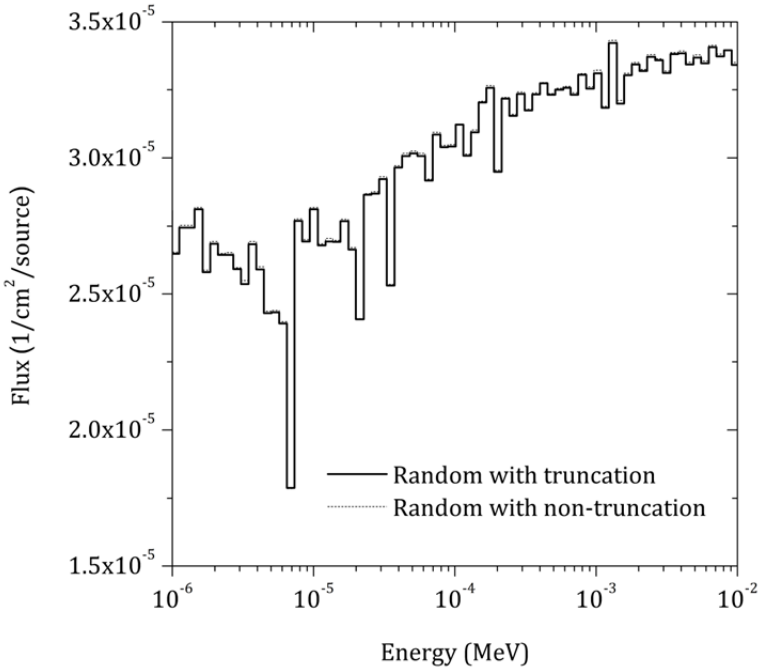

Fig. 5.5 Comparison of neutron flux in the resonance region between truncation and non-truncation models in the cases of random arrangement (#1)

国際単位系（SI）

表１．SI 基本単位

基本量	SI 基本単位	
	名称	記号
長さ	メートル	m
質量	キログラム	kg
時間	秒	s
電流	アンペア	A
熱力学温度	ケルビン	K
物質量	モル	mol
光度	カンデラ	cd

表２．基本単位を用いて表されるSI組立単位の例

組立量	SI 組立単位	
	名称	記号
面積	平方メートル	m^2
体積	立方メートル	m^3
速さ，速度	メートル毎秒	m/s
加速度	メートル毎秒毎秒	m/s^2
波数	毎メートル	m^{-1}
密度，質量密度	キログラム毎立方メートル	kg/m^3
面積密度	キログラム毎平方メートル	kg/m^2
比体積	立方メートル毎キログラム	m^3/kg
電流密度	アンペア毎平方メートル	A/m^2
磁界の強さ	アンペア毎メートル	A/m
量濃度(a)，濃度	モル毎立方メートル	mol/m^3
質量濃度	キログラム毎立方メートル	kg/m^3
輝度	カンデラ毎平方メートル	cd/m^2
屈折率(b)	（数字の） 1	1
比透磁率(b)	（数字の） 1	1

(a) 量濃度（amount concentration）は臨床化学の分野では物質濃度（substance concentration）ともよばれる。
(b) これらは無次元量あるいは次元１をもつ量であるが、そのことを表す単位記号である数字の１は通常は表記しない。

表３．固有の名称と記号で表されるSI組立単位

組立量	SI 組立単位			
	名称	記号	他のSI単位による表し方	SI基本単位による表し方
平面角	ラジアン(b)	rad	1 (b)	m/m
立体角	ステラジアン(b)	sr(c)	1 (b)	m^2/m^2
周波数	ヘルツ(d)	Hz		s^{-1}
力	ニュートン	N		$m\ kg\ s^{-2}$
圧力，応力	パスカル	Pa	N/m^2	$m^{-1}\ kg\ s^{-2}$
エネルギー，仕事，熱量	ジュール	J	N m	$m^2\ kg\ s^{-2}$
仕事率，工率，放射束	ワット	W	J/s	$m^2\ kg\ s^{-3}$
電荷，電気量	クーロン	C		s A
電位差（電圧），起電力	ボルト	V	W/A	$m^2\ kg\ s^{-3}\ A^{-1}$
静電容量	ファラド	F	C/V	$m^{-2}\ kg^{-1}\ s^4\ A^2$
電気抵抗	オーム	Ω	V/A	$m^2\ kg\ s^{-3}\ A^{-2}$
コンダクタンス	ジーメンス	S	A/V	$m^{-2}\ kg^{-1}\ s^3\ A^2$
磁束	ウエーバ	Wb	Vs	$m^2\ kg\ s^{-2}\ A^{-1}$
磁束密度	テスラ	T	Wb/m^2	$kg\ s^{-2}\ A^{-1}$
インダクタンス	ヘンリー	H	Wb/A	$m^2\ kg\ s^{-2}\ A^{-2}$
セルシウス温度	セルシウス度(e)	℃		K
光束	ルーメン	lm	cd sr(c)	cd
照度	ルクス	lx	lm/m^2	m^{-2} cd
放射性核種の放射能(f)	ベクレル(d)	Bq		s^{-1}
吸収線量，比エネルギー分与，カーマ	グレイ	Gy	J/kg	$m^2\ s^{-2}$
線量当量，周辺線量当量，方向性線量当量，個人線量当量	シーベルト(g)	Sv	J/kg	$m^2\ s^{-2}$
酸素活性	カタール	kat		s^{-1} mol

(a)SI接頭語は固有の名称と記号を持つ組立単位と組み合わせても使用できる。しかし接頭語を付した単位はもはやコヒーレントではない。
(b)ラジアンとステラジアンは数字の１に対する単位の特別な名称で、量についての情報をつたえるために使われる。実際には、使用する時には記号radおよびsrが用いられるが、習慣として組立単位としての記号である数字の１は明示されない。
(c)測光学ではステラジアンという名称と記号srを単位の表し方の中に、そのまま維持している。
(d)ヘルツは周期現象についてのみ、ベクレルは放射性核種の統計的過程についてのみ使用される。
(e)セルシウス度はケルビンの特別な名称で、セルシウス温度を表すために使用される。セルシウス度とケルビンの単位の大きさは同一である。したがって、温度差や温度間隔を表す数値はどちらの単位で表しても同じである。
(f)放射性核種の放射能（activity referred to a radionuclide）は、しばしば誤った用語で"radioactivity"と記される。
(g)単位シーベルト（PV,2002,70,205）についてはCIPM勧告2（CI-2002）を参照。

表４．単位の中に固有の名称と記号を含むSI組立単位の例

組立量	SI 組立単位		
	名称	記号	SI 基本単位による表し方
粘度	パスカル秒	Pa s	$m^{-1}\ kg\ s^{-1}$
力のモーメント	ニュートンメートル	N m	$m^2\ kg\ s^{-2}$
表面張力	ニュートン毎メートル	N/m	$kg\ s^{-2}$
角速度	ラジアン毎秒	rad/s	$m\ m^{-1}\ s^{-1}=s^{-1}$
角加速度	ラジアン毎秒毎秒	rad/s^2	$m\ m^{-1}\ s^{-2}=s^{-2}$
熱流密度，放射照度	ワット毎平方メートル	W/m^2	$kg\ s^{-3}$
熱容量，エントロピー	ジュール毎ケルビン	J/K	$m^2\ kg\ s^{-2}\ K^{-1}$
比熱容量，比エントロピー	ジュール毎キログラム毎ケルビン	J/(kg K)	$m^2\ s^{-2}\ K^{-1}$
比エネルギー	ジュール毎キログラム	J/kg	$m^2\ s^{-2}$
熱伝導率	ワット毎メートル毎ケルビン	W/(m K)	$m\ kg\ s^{-3}\ K^{-1}$
体積エネルギー	ジュール毎立方メートル	J/m^3	$m^{-1}\ kg\ s^{-2}$
電界の強さ	ボルト毎メートル	V/m	$m\ kg\ s^{-3}\ A^{-1}$
電荷密度	クーロン毎立方メートル	C/m^3	m^{-3} s A
表面電荷	クーロン毎平方メートル	C/m^2	m^{-2} s A
電束密度，電気変位	クーロン毎平方メートル	C/m^2	m^{-2} s A
誘電率	ファラド毎メートル	F/m	$m^{-3}\ kg^{-1}\ s^4\ A^2$
透磁率	ヘンリー毎メートル	H/m	$m\ kg\ s^{-2}\ A^{-2}$
モルエネルギー	ジュール毎モル	J/mol	$m^2\ kg\ s^{-2}\ mol^{-1}$
モルエントロピー，モル熱容量	ジュール毎モル毎ケルビン	J/(mol K)	$m^2\ kg\ s^{-2}\ K^{-1}\ mol^{-1}$
照射線量（X線及びγ線）	クーロン毎キログラム	C/kg	kg^{-1} s A
吸収線量率	グレイ毎秒	Gy/s	$m^2\ s^{-3}$
放射強度	ワット毎ステラジアン	W/sr	$m^4\ m^{-2}\ kg\ s^{-3}=m^2\ kg\ s^{-3}$
放射輝度	ワット毎平方メートル毎ステラジアン	$W/(m^2\ sr)$	$m^2\ m^{-2}\ kg\ s^{-3}=kg\ s^{-3}$
酵素活性濃度	カタール毎立方メートル	kat/m^3	$m^{-3}\ s^{-1}$ mol

表５．SI 接頭語

乗数	名称	記号	乗数	名称	記号
10^{24}	ヨタ	Y	10^{-1}	デシ	d
10^{21}	ゼタ	Z	10^{-2}	センチ	c
10^{18}	エクサ	E	10^{-3}	ミリ	m
10^{15}	ペタ	P	10^{-6}	マイクロ	μ
10^{12}	テラ	T	10^{-9}	ナノ	n
10^9	ギガ	G	10^{-12}	ピコ	p
10^6	メガ	M	10^{-15}	フェムト	f
10^3	キロ	k	10^{-18}	アト	a
10^2	ヘクト	h	10^{-21}	ゼプト	z
10^1	デカ	da	10^{-24}	ヨクト	y

表６．SIに属さないが、SIと併用される単位

名称	記号	SI 単位による値
分	min	1 min=60 s
時	h	1 h =60 min=3600 s
日	d	1 d=24 h=86 400 s
度	°	1°=(π/180) rad
分	’	1’=(1/60)°=(π/10 800) rad
秒	”	1”=(1/60)’=(π/648 000) rad
ヘクタール	ha	1 ha=1 $hm^2=10^4m^2$
リットル	L, l	1 L=1 l=1 $dm^3=10^3cm^3=10^{-3}m^3$
トン	t	1 t=10^3 kg

表７．SIに属さないが、SIと併用される単位で、SI単位で表される数値が実験的に得られるもの

名称	記号	SI 単位で表される数値
電子ボルト	eV	1 eV=1.602 176 53(14)×10^{-19}J
ダルトン	Da	1 Da=1.660 538 86(28)×10^{-27}kg
統一原子質量単位	u	1 u=1 Da
天文単位	ua	1 ua=1.495 978 706 91(6)×10^{11}m

表８．SIに属さないが、SIと併用されるその他の単位

名称	記号	SI 単位で表される数値
バール	bar	1 bar=0.1MPa=100 kPa=10^5Pa
水銀柱ミリメートル	mmHg	1 mmHg≈133.322Pa
オングストローム	Å	1 Å=0.1nm=100pm=10^{-10}m
海里	M	1 M=1852m
バーン	b	1 b=100fm^2=$(10^{-12}cm)^2$=$10^{-28}m^2$
ノット	kn	1 kn=(1852/3600)m/s
ネーパ	Np	SI単位との数値的な関係は、対数量の定義に依存。
ベル	B	
デシベル	dB	

表９．固有の名称をもつCGS組立単位

名称	記号	SI 単位で表される数値
エルグ	erg	1 erg=10^{-7} J
ダイン	dyn	1 dyn=10^{-5}N
ポアズ	P	1 P=1 dyn s cm^{-2}=0.1Pa s
ストークス	St	1 St =1$cm^2\ s^{-1}$=$10^{-4}m^2\ s^{-1}$
スチルブ	sb	1 sb =1cd cm^{-2}=10^4cd m^{-2}
フォト	ph	1 ph=1cd sr cm^{-2} =10^4lx
ガル	Gal	1 Gal =1cm s^{-2}=$10^{-2}ms^{-2}$
マクスウエル	Mx	1 Mx = 1G cm^2=10^{-8}Wb
ガウス	G	1 G =1Mx cm^{-2} =10^{-4}T
エルステッド(a)	Oe	1 Oe ≙ $(10^3/4\pi)$A m^{-1}

(a) ３元系のCGS単位系とSIでは直接比較できないため、等号「 ≙ 」は対応関係を示すものである。

表10．SIに属さないその他の単位の例

名称	記号	SI 単位で表される数値
キュリー	Ci	1 Ci=3.7×10^{10}Bq
レントゲン	R	1 R = 2.58×10^{-4}C/kg
ラド	rad	1 rad=1cGy=10^{-2}Gy
レム	rem	1 rem=1 cSv=10^{-2}Sv
ガンマ	γ	1 γ=1 nT=10^{-9}T
フェルミ		1 フェルミ=1 fm=10^{-15}m
メートル系カラット		1 メートル系カラット= 0.2 g = 2×10^{-4}kg
トル	Torr	1 Torr = (101 325/760) Pa
標準大気圧	atm	1 atm = 101 325 Pa
カロリー	cal	1 cal=4.1858J（「15℃」カロリー），4.1868J（「IT」カロリー），4.184J（「熱化学」カロリー）
ミクロン	μ	1 μ =1μm=10^{-6}m

（第8版，2006年）